AFOSR - TR - 76 - 0332

AFOSR 71-2145

S. R. No. 7

November, 1975

Technion Research & Development Foundation Ltd.
Haifa, Israel

FC

12

See 1473

ADA023147

SCIENTIFIC REPORT No. 7

THE INITIAL ROLL-UP OF A THICK, TWO-DIMENSIONAL WAKE BEHIND A WING OF FINITE SPAN

BY

H. PORTNOY

Department of Aeronautical Engineering
Technion — Israel Institute of Technology
Haifa, Israel

T.A.E. REPORT No. 262

AF OSR 71-2145

S.R. No. 7.

NOVEMBER, 1975

SCIENTIFIC REPORT No. 7.

THE INITIAL ROLL-UP OF A THICK,TWO-DIMENSIONAL WAKE BEHIND A WING OF FINITE SPAN.

by

H. PORTNOY
Department of Aeronautical Engineering,
Technion - Israel Institute of Technology,
Haifa, Israel.

TAE REPORT No. 262

ABSTRACT

Previous investigations of wing-wake roll-up have assumed the wake to be a vortex sheet of zero thickness. This immediately leads to the conclusion that, as soon as the process starts, a spiral of near axisymmetric form, with an infinite number of turns, forms at the edge, as predicted by the work of Kaden, which must apply to the early stages of roll-up for any sheet of zero thickness. In addition, most investigators, starting with Westwater, have replaced the continuous vortex sheet by discrete vortex lines.

In this report, the aforementioned unrealistic features are removed by assuming that the wake cross-section has a finite thickness and some plausible shape. A two-dimensional method, analogous to that of Westwater, is developed, assuming that the wake cross-section contains vorticity in an otherwise irrotational field. The wake is divided into triangular elements and the vorticity in these is determined by assuming a linear transverse velocity profile in the wake and that the initial, unrolled wake moves downwards as determined by the wing spanwise loading through ordinary wing-wake theory. Euler time-step integration is then used to calculate the wake development under its own induced velocity field, ignoring viscous dissipation.

Three examples of the initial stages of roll-up, for elliptic wakes of thickness ratios .04, .05 and .06, are calculated. A finite spiral structure is observed to develop and, within the range covered, the thickness only seems to affect the number of turns in the spiral, other parameters seeming to be almost unaffected.

Plans for continuation of the work are discussed.

TABLE OF CONTENTS

LIST OF SYMBOLS

A	wake cross-section at any station x.
A'	initial wake cross-section at $x = 0$.
AR	aspect ratio of wing.
a	side of triangular element, opposite corner A, divided by s.
b	side of triangular element, opposite corner B, divided by s.
C	boundary of cross-section A.
C'	boundary of cross-section A'.
C_L	wing lift coefficient.
c	side of triangular element, opposite corner C, divided by s.
K_n	$=\xi_n^* \Delta A_n^*$.
M	total number of triangular elements in wake cross-section.
N	number of different values of ξ_n^* .
n	number denoting a typical triangular element.
P	perimeter of S.
r_A	$= \lvert\zeta - \zeta_A\rvert/s$.
r_B	$= \lvert\zeta - \zeta_B\rvert/s$.
r_C	$= \lvert\zeta - \zeta_C\rvert/s$.
S	closed region with constant vorticity distribution.
s	wing semi-span.
t^*	dimensionless time. See Equation (4).
U	free stream velocity.
V_n	element influence function. See Equation (14).
v	velocity component in the y direction.
v^*	non-dimensional form of v. See Equation (3).

W_n	element influence function. See Equation (15).
w	velocity component in the z direction.
w^*	non-dimensional form of w. See Equation (3).
w_I^*	$-w_I^*$ is the usual downwash calculated in the Treffz plane for an unrolled wake.
x	streamwise coordinate.
y	spanwise coordinate positive to the right.
y^*	$= y/s$.
z	third coordinate of the right-handed set x, y, z.
z^*	$= z/s$.
α	$= \arg (\zeta - \zeta_A)$.
α_B	$= \arg (\zeta_B - \zeta_A)$.
α_C	$= \arg (\zeta_C - \zeta_A)$.
β	$= \arg (\zeta - \zeta_B)$.
β_A	$= \arg (\zeta_A - \zeta_B)$.
β_C	$= \arg (\zeta_C - \zeta_B)$.
γ	$= \arg (\zeta - \zeta_C)$.
γ_A	$= \arg (\zeta_A - \zeta_C)$.
γ_B	$= \arg (\zeta_B - \zeta_C)$.
ΔA_n	area of nth triangular element.
ΔA_n^*	$= \Delta A_n/s^2$.
Δt^*	dimensionless time step in numerical integration.
Δv_n^*	contribution to v^* from nth triangular element.
Δw_n^*	contribution to w^* from nth triangular element.

ε	thickness ratio of elliptic wake cross-section.
ζ	$= y + iz$.
ζ_A	ζ at corner A of nth element.
ζ_B	ζ at corner B of nth element.
ζ_C	ζ at corner C of nth element.
θ	$= \cos^{-1} y^*$.
λ	$= \tan^{-1}(dz^*/dy^*)_{C'}$.
$\xi(z,y,z)$	vorticity distribution within A .
$\xi^*(t^*,y^*,z^*)$	non-dimensional form of ξ. See Equation (5).
ξ_n	constant value of ξ in nth triangle.
ξ_n^*	non-dimensional form of ξ_n .
ξ_s	constant value of ξ inside S.
$\omega(y)$	vorticity distribution within A'.
$\omega^*(y^*)$	non-dimensional form of ω. See Equation (5).

1. INTRODUCTION

Many investigators have studied the rolling-up of the vortex wake behind a wing of finite span. The earliest step in this study was the work of Kaden[1] who found an analytical solution for the rolling-up with time of a semi-infinite, straight, two-dimensional vortex sheet. This solution must represent the situation very close to the edges of a finite-span vortex sheet of zero thickness, in two or three dimensions, during the initial stage of the rolling-up process. An important result following from Kaden's work is that, from the very onset of rolling-up, due to the infinite velocity at the sheet edge, a spiral of near-axi-symmetric form, with an infinite number of turns, is established at the edge. This is a consequence of the assumption of zero thickness for the sheet.

Westwater[2] considered a finite-span, zero-thickness wake resulting from an elliptically-loaded wing and assumed that the roll-up could be treated as a two-dimensional time-dependent process, where the configurations at successive stages in time represent successively further downstream sections of the wake, as fixed by the forward speed of the wing multiplied by the time. This approach is evidently suitable for wakes which roll up relatively slowly far behind the wing, such as are found with high-aspect-ratio, unswept wings. Westwater further simplified his calculations by replacing the continuous vortex sheet by a row of infinite line vortices. Clements and Maull[3] have recently used this technique for non-elliptic span-loadings. Westwater's method is subject to certain numerical difficulties which have been the subject of a number of investigations. A particularly careful recent review and study of this matter is due to Moore[4], who develops a method for overcoming the problem.

The line-vortex method has been extended to cover three-dimensional effects, such as those of bound vorticity and the finite origin and stream-wise curvature of the trailing vortices, by the use of the vortex-lattice procedure[5,6,7,8,9]. This leads to results applicable to low-aspect-ratio and swept wings.

The present work is an attempt to remove the unrealistic features of the earlier models, namely zero wake thickness and vorticity concentrated on lines, by assuming that the wake vorticity is contained in a layer of finite thickness with some plausible cross-sectional shape. The wake flow is assumed to be two-dimensional and the rolling- up is studied via the time-dependent development of this model, exactly as in Westwater's work, so that we deal with a slow rolling-up taking place far behind the wing, once more. The introduction of vorticity distributed continuously throughout the wake cross-section enables us to obtain a more acceptable picture of the initial rolling up phase than the infinite spiral of Kaden.

Having selected an appropriate wake cross-section its area is divided into triangular elements within each of which the vorticity is assumed constant, and for which simple expressions giving the velocity field have been derived (see Section 3). The strength of the vorticity within each triangle is determined using two assumptions:

(1) The vorticity is constant through the wake thickness. This corresponds to an assumption that the transverse velocity profile within the wake is linear.

(2) The periphery of the wake is moving downwards with a velocity determined by spanwise position and wing spanwise loading, exactly as in ordinary wing-wake theory.

Assumption (1) can evidently be removed at the cost of increasing the number of triangular elements used.

Once the triangle strengths are found, the network of points defining the wake is allowed to distort with time under its self-induced velocity field, using Euler integration. During this process viscous dissipation is neglected, so that the vorticity inside each triangle remains constant, as will its area (due to continuity), even though the shape changes.

Examples of the initial roll-up phase have been calculated for three wakes of different thicknesses and elliptic cross-sections, subjected to uniform downwash (corresponding to elliptic spanwise loading). Details and results are given in Sections 5 and 6, and plans for future work in Section 7.

2. THE MATHEMATICAL MODEL

The mathematical model of the wake and the notation are illustrated in Fig. 1.

The unrolled wake cross-section A', whose boundary is denoted by C', stretches between $y = -s$ and $y = +s$ in the plane $x = 0$. At subsequent stations $x = x$, the boundary is denoted by C and the wake has a rolled up form of cross section A with vorticity distribution $\xi(x,y,z)$ determined by the original configuration of the wake cross-section, the original vorticity distribution within it, $\xi(0,y,z)$, and the elapsed time x/U. It is assumed that

$$\xi(0,y,z) = \omega(y) \quad , \tag{1}$$

corresponding to a linear variation with z of the velocity, v, within the initial wake section, if the wake is assumed thin.

We define dimensionless coordinates

$$y^* = \frac{y}{s} \quad ; \quad z^* = \frac{z}{s} \tag{2}$$

and since a typical velocity of the flow in the wake cross-sectional plane is $\frac{2UC_L}{\pi . AR}$, we also define dimensionless velocity components, time and vorticity by

$$v^* = \frac{\pi AR.v}{2UC_L} \quad ; \quad w^* = \frac{\pi AR.w}{2UC_L} \quad , \tag{3}$$

$$t^* = \frac{2C_L x}{\pi . AR.s} \quad , \tag{4}$$

$$\omega^*(y^*) = \frac{\omega\ \pi . AR.s}{2UC_L} \quad ; \quad \xi^*(t^*,y^*,z^*) = \frac{\xi\pi . AR.s}{2UC_L} \quad . \tag{5}$$

We assume that ω or ω^* is determined by the boundary conditions:

(a) $$w^* \cos\lambda - v^* \sin\lambda = w_I^* (y^*)\cos\lambda \qquad (6)$$

on C'

where $(dz^*/dy^*)_{C'} = \tan\lambda$, and

(b) $$\sqrt{v^{*2} + w^{*2}} \to 0 \text{ as } \sqrt{y^{*2} + z^{*2}} \to \infty \; . \qquad (7)$$

$- w_I^* (y^*)$ is the non-dimensionalised downwash distribution in the Treffz plane as calculated from the usual unrolled thin-wake theory. For example, $w_I^* = -1$ for elliptic spanwise load distribution. It is readily shown that, in the general form, w_I^* is dependent on the form of the spanwise loading and y^* only (c.f. reference 3).

It now follows that for a given initial wake cross-section and spanwise loading, the velocities v^* and w^* of a given fluid particle are functions of t^* only, so that the subsequent non-dimensional coordinates of the particles constituting the rolled wake are functions of t^* only, determined by the differential equations

$$\frac{dy^*}{dt^*} = v^* \quad ; \quad \frac{dz^*}{dt^*} = w^* \; . \qquad (8)$$

The equations (8) are integrated numerically step by step, starting from the initial configuration, using Euler integration.

It remains to determine the velocity field (v^*, w^*) due to the distribution ξ^* within C.

3. THE VELOCITY FIELD

At any value of x, the two-dimensional velocity field, (v, w), is determined by integrating the effects of point vortices of strengths $\xi(x,y,z)\,dy\,dz$ over the area of the wake cross-section, A.

To facilitate the numerical calculations, A is divided into a finite number of small triangular elements within each of which the value of ξ is assumed constant. We now find expressions for Δv_n^* and Δw_n^* due to a typical element of this kind for points outside its boundary, or approaching the boundary in a limiting sense. This enables us to calculate v^* and w^* for the assemblage of triangles at all the node points of the triangular mesh, including internal nodes of A, since such points may be regarded as being inside infinitesimal cavities excluded from all the adjacent triangles, and we calculate, in effect, the principal value of the velocity integral - which is precisely the required definition of this integral inside the vorticity distribution.

The velocity field outside any area S containing a constant vorticity distribution, ξ_S, may be written

$$v - iw = \frac{-i\xi_S}{2\pi} \iint_S \frac{dy_1\,dz_1}{y + iz - y_1 - iz_1} \quad . \qquad (9)$$

Using Green's theorem, this may be converted to a line integral around P, the perimeter of S:

$$v - iw = \frac{i\xi_S}{2\pi} \int_P \ln(\zeta - y_1 - iz_1)\,dy_1 \qquad (10)$$

where $\zeta = y + iz$.

If (10) is applied to a typical triangle of A, of area ΔA_n, vorticity distribution strength ξ_n and vertices defined by ζ_A, ζ_B, ζ_C (Fig. 2), we obtain

$$\Delta v_n - i\Delta w_n = -\frac{-i\xi_n\Delta A_n}{\pi}\left\{\frac{\zeta-\zeta_A}{(\zeta_C-\zeta_A)(\zeta_B-\zeta_A)}\ln(\zeta-\zeta_A) + \right.$$

$$\left. + \frac{\zeta-\zeta_B}{(\zeta_C-\zeta_B)(\zeta_A-\zeta_B)}\ln(\zeta-\zeta_B) + \frac{\zeta-\zeta_C}{(\zeta_A-\zeta_C)(\zeta_B-\zeta_C)}\ln(\zeta-\zeta_C)\right\} . \tag{11}$$

ξ_n and ΔA_n are both invariant with the motion for an infinitesimal triangle in incompressible flow, the product $\xi_n\Delta A_n$ being the circulation around the element.

If we now write $s^2\Delta A_n^* = \Delta A_n$, then

$$\xi_n\Delta A_n = \frac{2UsC_L}{\pi AR}\xi_n^*\Delta A_n^* = \frac{2UsC_L}{\pi AR}K_n \tag{12}$$

and if (see Fig. 2)

$$\left.\begin{array}{llll}
\zeta-\zeta_A = sr_Ae^{i\alpha} & ; \quad \zeta-\zeta_B = sr_Be^{i\beta} & ; \quad \zeta-\zeta_C = sr_Ce^{i\gamma} \\
\zeta_B-\zeta_A = sce^{i\alpha_B} & ; \quad \zeta_C-\zeta_A = sbe^{i\alpha_C} & \\
\zeta_C-\zeta_B = sae^{i\beta_C} & ; \quad \zeta_A-\zeta_B = sce^{i\beta_A} & \\
\zeta_A-\zeta_C = sbe^{i\gamma_A} & \quad\;\; \zeta_B-\zeta_C = sae^{i\gamma_B} &
\end{array}\right\} \tag{13}$$

we obtain from (11)

$$\begin{aligned}
\Delta v_n^* = \frac{K_n}{\pi}\Big\{&\frac{r_A}{bc}[\sin(\alpha-\alpha_C-\alpha_B)\ln r_A + \alpha\cos(\alpha-\alpha_C-\alpha_B)] + \\
&+ \frac{r_B}{ca}[\sin(\beta-\beta_C-\beta_A)\ln r_B + \beta\cos(\beta-\beta_C-\beta_A)] + \\
&+ \frac{r_C}{ab}[\sin(\gamma-\gamma_A-\gamma_B)\ln r_C + \gamma\cos(\gamma-\gamma_A-\gamma_B)]\Big\} \\
= K_nV_n(y^*,z^*)&
\end{aligned} \tag{14}$$

$$\Delta w_n^* = \frac{K_n}{\pi}\left\{\frac{r_A}{bc}[\cos(\alpha-\alpha_C-\alpha_B)\ln r_A - \alpha\sin(\alpha-\alpha_C-\alpha_B)] + \right.$$

$$+ \frac{r_B}{ca}[\cos(\beta-\beta_C-\beta_A)\ln r_B - \beta\sin(\beta-\beta_C-\beta_A)] +$$

$$\left. + \frac{r_C}{ab}[\cos(\gamma-\gamma_A-\gamma_B)\ln r_C - \gamma\sin(\gamma-\gamma_A-\gamma_B)]\right\}$$

$$= K_n W_n(y^*,z^*) \quad . \tag{15}$$

Hence we have the approximations

$$v^* \approx \sum_{n=1}^{M} K_n V_n(y^*,z^*) \tag{16}$$

$$w^* \approx \sum_{n=1}^{M} K_n W_n(y^*,z^*) \quad . \tag{17}$$

4. THE NUMERICAL PROCEDURE

Because of the spanwise symmetry of the initial cross-section, A', and the assumption (1), the M values of K_n are dependent on a smaller number of values of ξ_n^*, say N. The boundary condition (6) is now applied at N suitable node points on the initial boundary A' (excluding the tip points), using the expressions (16) and (17), with unknown coefficients, $K_n = \xi_n^* A_n^*$, thus yielding N linear equations for the ξ_n^* and hence the K_n. The equations (16) and (17) may now be used to evaluate v^* and w^* at all values of t^*, once the dimensionless coordinates of the triangles are known. These are found step by step by numerical integration of the equations (8) forward in time t^*, starting with the known initial set of triangles within A'. The development of the wake roll-up is thus calculated step by step. The y^* coordinate of the "centroid" of vorticity of one half of the wake is calculated at each step. This should remain constant[10] and provides an accuracy check.

5. THE WAKE OF ELLIPTIC CROSS-SECTION SUBJECT TO UNIFORM DOWNWASH

In this case the equation of C' is

$$z^* = \pm \varepsilon\sqrt{1 - y^{*2}} \tag{18}$$

and

$$w_I^* = -1 . \tag{19}$$

Also

$$\tan\lambda = \mp \frac{\varepsilon y^*}{\sqrt{1 - y^{*2}}} . \tag{20}$$

The cross-section A' is divided into triangular elements as shown in Figure 3. It was found necessary to concentrate the triangles near the tips. This was done as follows. Firstly a basic set of spanwise stations was established by using an even number of equal divisions of the eccentric angle coordinate

$$\theta = \cos^{-1} y^* \tag{21}$$

across the span. Next, the segment at the tip was further subdivided into two equal θ intervals and all resulting divisions were then again subdivided into two for a specified number of the segments, starting from the tips and moving inboard. Using the horizontal diameter of the ellipse as another division line, triangles may then be filled in as shown in Figure 3. ξ_n^* is taken as constant over the four triangles lying between any two vertical lines (at the tip - over two triangles) and the same value is taken for the symmetrically placed group on the other half wake. In the illustration, the spanwise subdivision is 8 + 2 + 6, the number of triangles is 60 and the number of different values of ξ_n^* is 8. The points for applying the boundary condition are shown circled.

An analytic solution exists for the downward moving elliptic cylinder, which corresponds to the flow at $t^* = 0$. The flow calculated by the present method at $t^* = 0$ was compared to this for the three cases considered, namely, $\varepsilon = .04$, .05 and .06. In all these cases, a subdivision of 40 + 2 + 8 spanwise gave results for surface velocity, total amount of vorticity in one half wake and spanwise position of centroid, which were considered to compare adequately with the theoretical values and this distribution of points was also found to be just adequate for describing the spiral structure of the core up to the time reached in the calculation of the roll-up. During the roll-up, the centroid position spanwise remained constant to a high degree of accuracy for the range covered (change not more than 1 part in 780). The total times covered were $t^* = .0128$, .0160 and .0192 for the thickness ratios .04, .05 and .06, respectively.

The appearance of the tip region is shown for various stages of this initial roll-up in Figures 4,5, and 6 for $\varepsilon = .04$, .05 and .06, respectively and in Figure 7 one example of a complete half-wake is shown. It should be noted that to clarify the inner detail of the spiral, the vertical scale has been exaggerated in these figures and this vertical scale is not uniform throughout all the pictures. The results are discussed in the next Section.

6. DISCUSSION AND RESULTS

The time step, Δt^*, used in the numerical integration was found to be a critical parameter in the calculation, whereas the results were not very sensitive to spanwise divisions, provided sufficient were present near the tip to ensure enough points, at close enough spacings, to describe the spiral structure. After some experiment, it was found that the 40 + 2 + 8 subdivision gave results as good as those from larger numbers of cells, although the need for further points near the tip does not become evident at later stages in the spiral development.

As regards Δt^*, if this is taken very small, chaotic motion of the points can develop after a large number of small steps have been taken during the initial short period of high distortion rate of the wake tip. This effect, which is not so critical later on in the calculation, appears to be due to accumulated errors resulting from neglect of the distortions of the triangular elements at each step, distortions which makes them increasingly curvilinear in reality. On the other hand, too large a Δt^* leads to incorrect wake shapes which are not substantiated on reduction of the time step. There seems to be an optimum Δt^* for each thickness ratio which avoids chaotic motion and for which the wake shape is relatively invariant with modest changes of this time step.

Another difficulty which occurred was overlap of triangular elements (an event formally violating the equation of continuity of the motion). This occurred either near the beginning of the roll-up, when the spiral tip, turning inwards, occasionally crossed onto the main body of the wake, or, later on, within the turns of the spiral. In the former case a cure could be effected by slightly decreasing Δt^*, and in the latter case more points should be incorporated near the tip. However, it was found impossible to increase the number of points sufficiently to completely remove overlap within the spiral during the later stages when the spiral coils stretch and wind up tightly. This is evidently a difficulty inherent in the use of straight-sided elements to represent a stretching spiral structure. It was found, however, that the shape of smooth spiral curves drawn through the node points was not greatly affected by the increase of points to avoid overlap, so it was concluded that the true, smooth spiral shape was still given fairly accurately by the node points even when a small amount of overlap occurred, provided that the pattern formed a logical extension of previous non-overlapping cases and that there was consistency between neighbouring lines of the coil,that is between the original center-line, which is shown dotted in the drawings, and the outer boundaries.

Using this approach, we are able to follow the up to one and three-quarter turns of the spiral, which occur in the present examples.

An analysis of the results shows that, for the range of thickness ratios covered, for the elliptic cross-sectioned wake:

(1) Thickness has little effect on the amount of vorticity within the core at a given t^* (Figure 8).

(2) Thickness has almost no effect on the size of the core at a given t^* (Figure 9).

(3) Except in the very initial stages of roll-up, the core is of an approximately elliptic shape with height/width ratio about 0.8 for all three thickness ratios studied (Figure 10).

(4) The number of turns of the spiral within the core at a given t^* increases with reduction of ε, except for very small values of t^* when the spiral is, in any case, ill-defined (Figure 11). About one and three-quarter turns are observed for the $\varepsilon = .04$ case at $t^* = .0128$ and for the $\varepsilon = .05$ case at $t^* = .0160$, and for the $\varepsilon = .06$ case at $t^* = .0192$, just over one and a half turns.

(5) An interesting result observed in all three cases is that the original tip point of the unrolled wake does not become the tip point of the spiral; instead it recedes back along the outer edge of the coil. This appears to be true also for subsequent tip points of the spiral - these do not remain at the tip but are dragged back along the outer edge of the spiral in their turn and their place is taken by other points which were originally more inboard along the upper edge of the unrolled wake.

7. FUTURE WORK

It is hoped to extend the present work into the more complete stages of the rolling-up and also to deal with different wake cross-sections and spanwise loadings.

For the later stages of the roll-up it would appear almost impossible to follow the spiral right into the center of the core and it is quite likely that considerable overlapping of elements may then occur there. Provided, however, that the outer winds of the spiral remain orderly and consistent, this need not trouble us, since what matters is the presence of the correct amount of vorticity in the core region, its precise location having little effect on the outer spiral. In effect we will be employing, automatically, the "condensing" procedure of Moore[4] wherebye the central part of the spiral is replaced by a point vortex.

Accuracy may, possibly, be improved by the use of curvilinear triangular elements instead of straight sided ones and also by use of a more sophisticated numerical integration method, such as the Runge-Kutta method.

ACKNOWLEDGMENTS

The author wishes to thank Mr. B. Fortune and Mrs. R. Gordon for help with the computer programming of this work.

REFERENCES

1. Kaden, H., Aufwicklung eines unstabilen Unstetigkeitsfläche. Ing. Archiv., Vol. 2, pp. 140-168., May 1931 (English translation R.A.E. Library Translation No. 403).
2. Westwater, F.L., The rolling up of the surface of discontinuity behind an aerofoil of finite span. British A.R.C. R and M 1692, 1935.
3. Clements, R.R., and Maull, D.J., The rolling of a trailing vortex sheet. The Aeronautical Journal, Vol. 77, No. 745, pp.46-51, Jan. 1973.
4. Moore, D.W., A numerical study of the roll-up of a finite vortex sheet. J. Fluid Mech., Vol. 63, Part 2, pp.225-235, 1974.
5. Hackett, J.F., and Evans, M.R., Vortex wakes behind high lift wings. Journal of Aircraft, Vol.8, No. 5, pp. 334-340, 1971.
6. Hancock, G.J., and Butter, D.J., A numerical method for calculating the trailing vortex system behind a swept wing at low speed. The Aeronautical Journal, Vol. 75, No. 728, pp. 564-568, 1971.
7. Rom, J., Zorea, C., and Gordon, R., On the calculation of non-linear aerodynamic characteristics and the near vortex wake. The 9th Congress of the ICAS, Haifa, Israel, ICAS paper No. 74-27, August 1974.
8. Labrujere, Th., E., A numerical method for the determination of the vortex sheet location behind a wing in incompressible flow. NLR TR 72091U, July 1972.
9. Maskew, B., The calculation of potential flow aerodynamics characteristics of combined lifting surfaces with relaxed wakes. Hawker-Siddeley Aviation Ltd., (Brough) Aerodynamic Design Dept. Note YAD 3192, Sept. 1973.
10. Betz, A. Verhalten von Wirbelsystemen, Z.A.M.M., Vol. 12, pp. 164-174, June 1932, (Also NACA TM 713, June 1933).

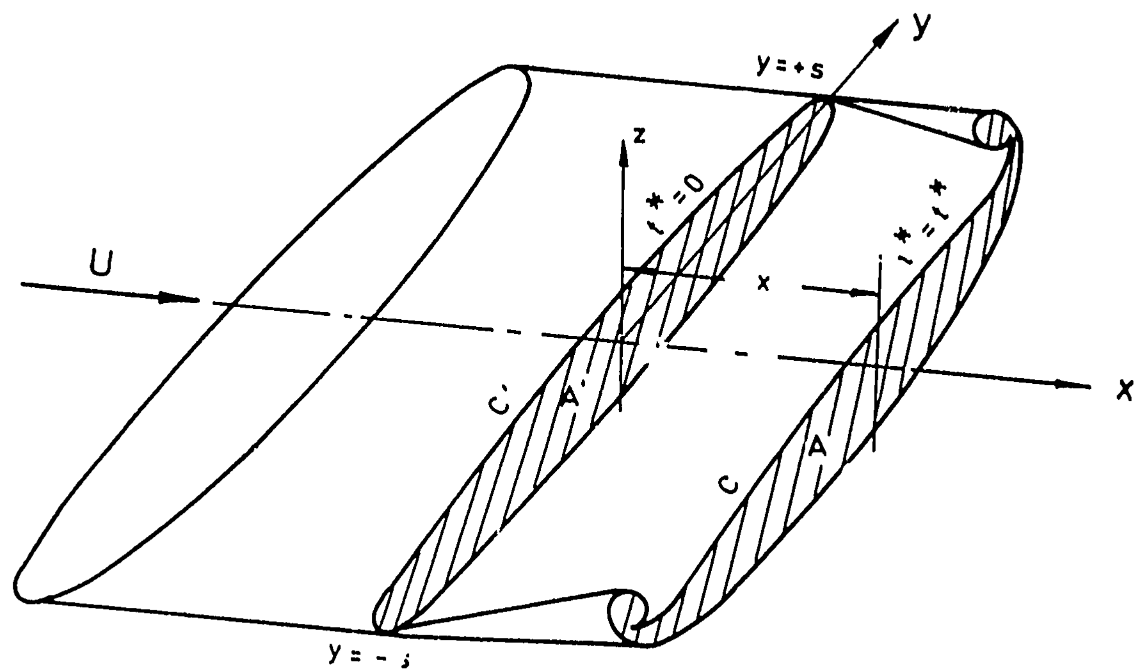

FIG.1 WAKE CROSS - SECTIONS & SYSTEM OF AXES.

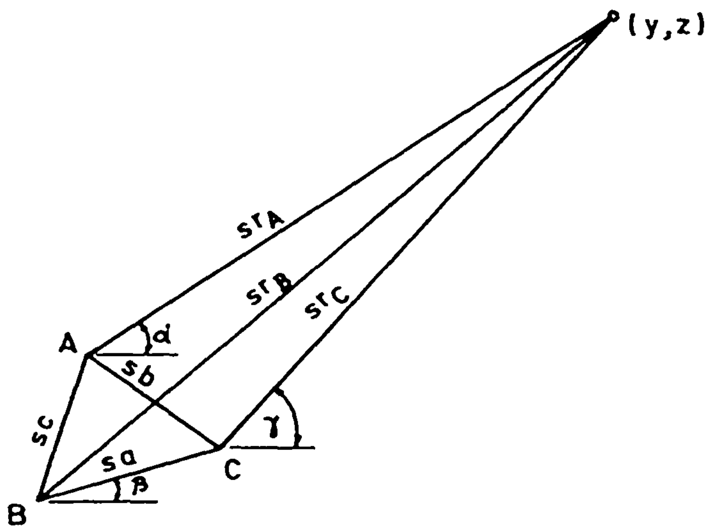

FIG.2 NOTATION FOR A TRIANGULAR ELEMENT & A FIELD POINT

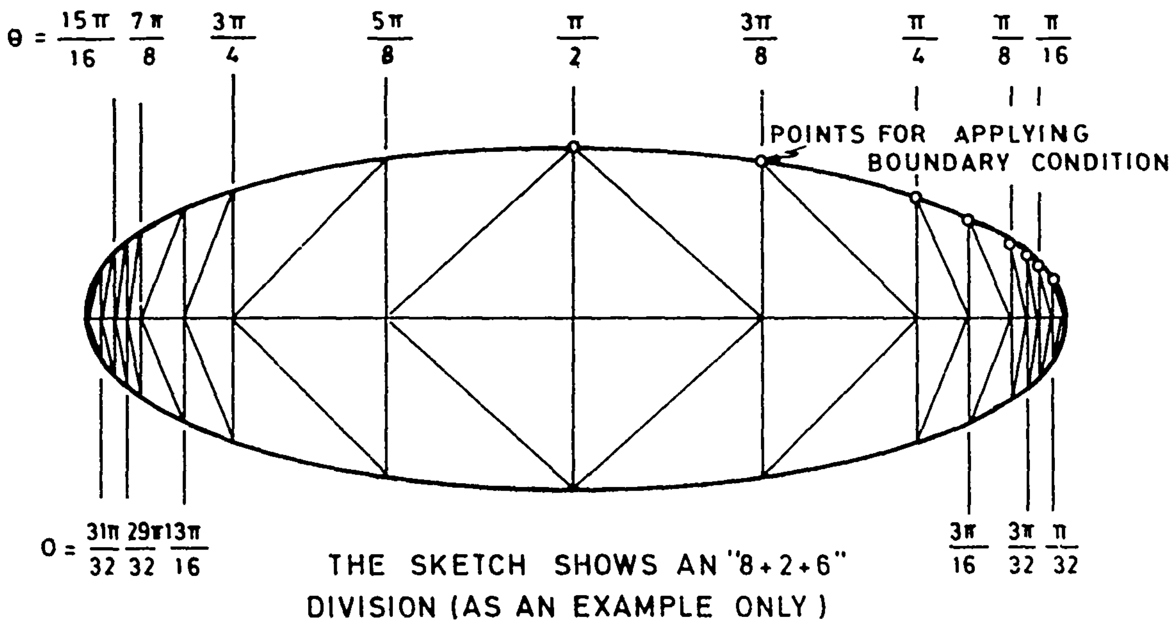

FIG. 3 LAYOUT OF ELEMENTS IN AN ELLIPTIC WAKE

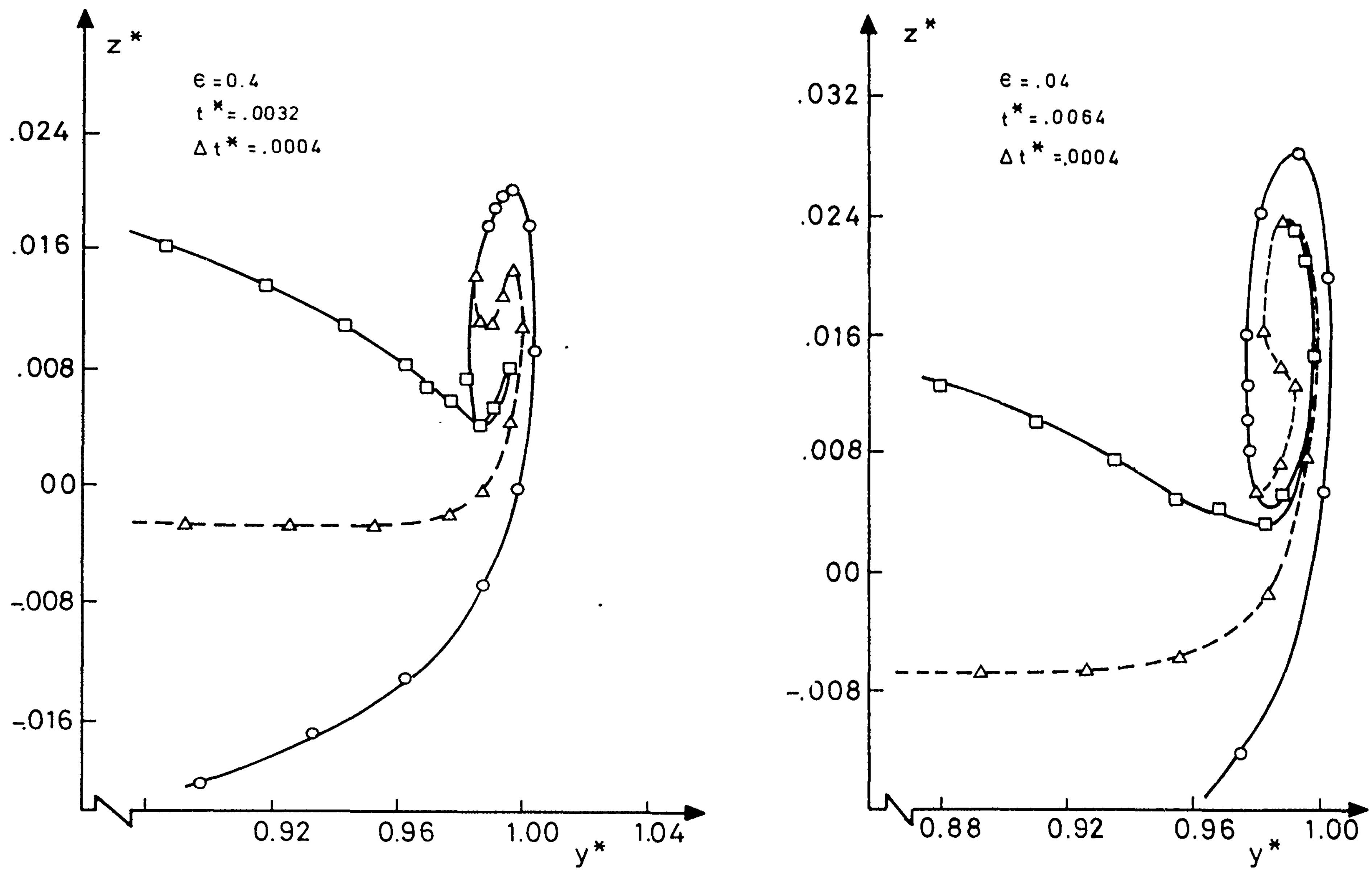

z*
ε = 0.4
t* = .0032
Δt* = .0004
.024
.016
.008
00
-.008
-.016
0.92
0.96
1.00
1.04
y*
z*
ε = .04
t* = .0064
Δt* = .0004
.032
.024
.016
.008
00
-.008
0.88
0.92
0.96
1.00
y*

FIG. 4

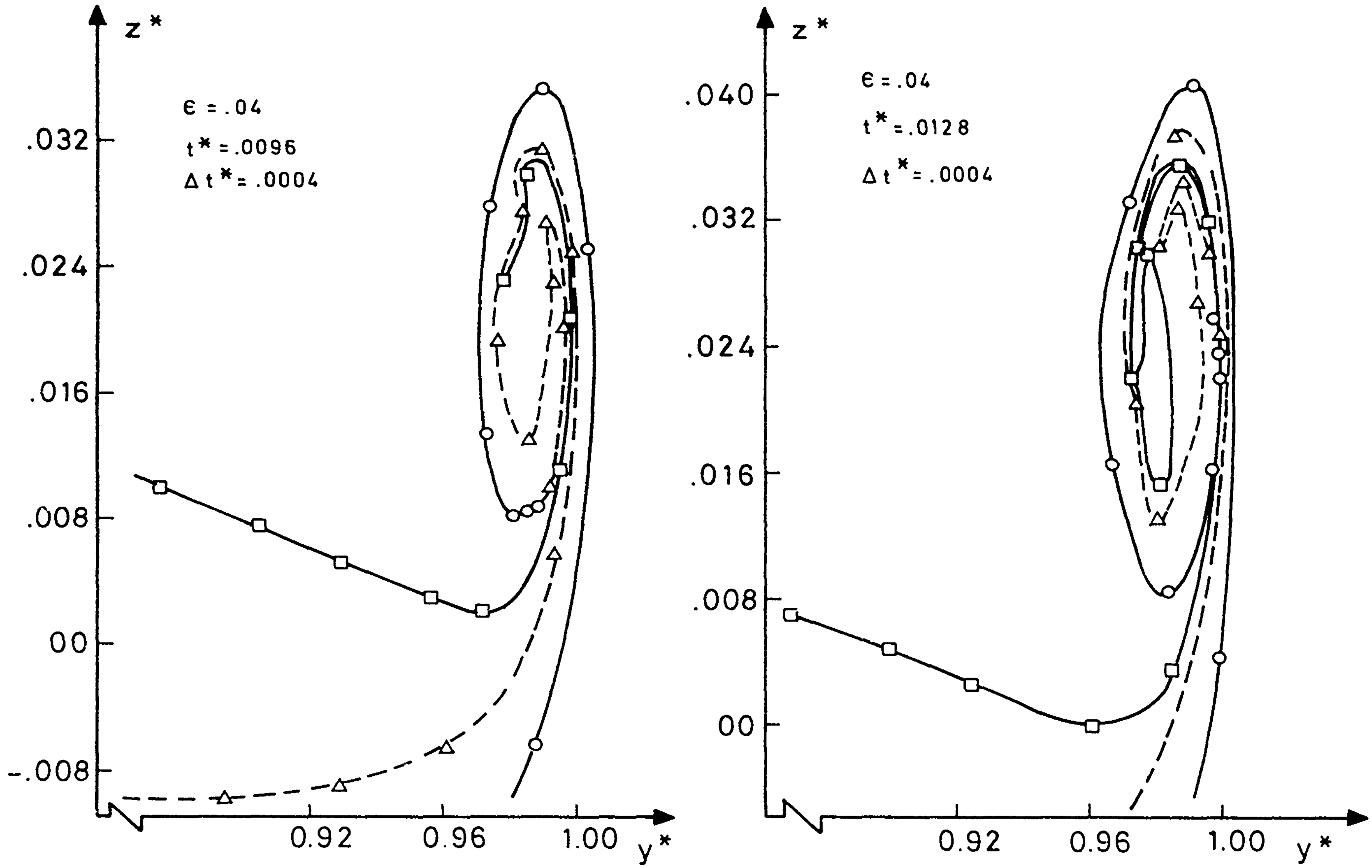

z*
ε = .04
t* = .0096
Δt* = .0004
.032
.024
.016
.008
00
-.008
0.92
0.96
1.00
y*
z*
ε = .04
t* = .0128
Δt* = .0004
.040
.032
.024
.016
.008
00
0.92
0.96
1.00
y*

FIG. 4 CONT.

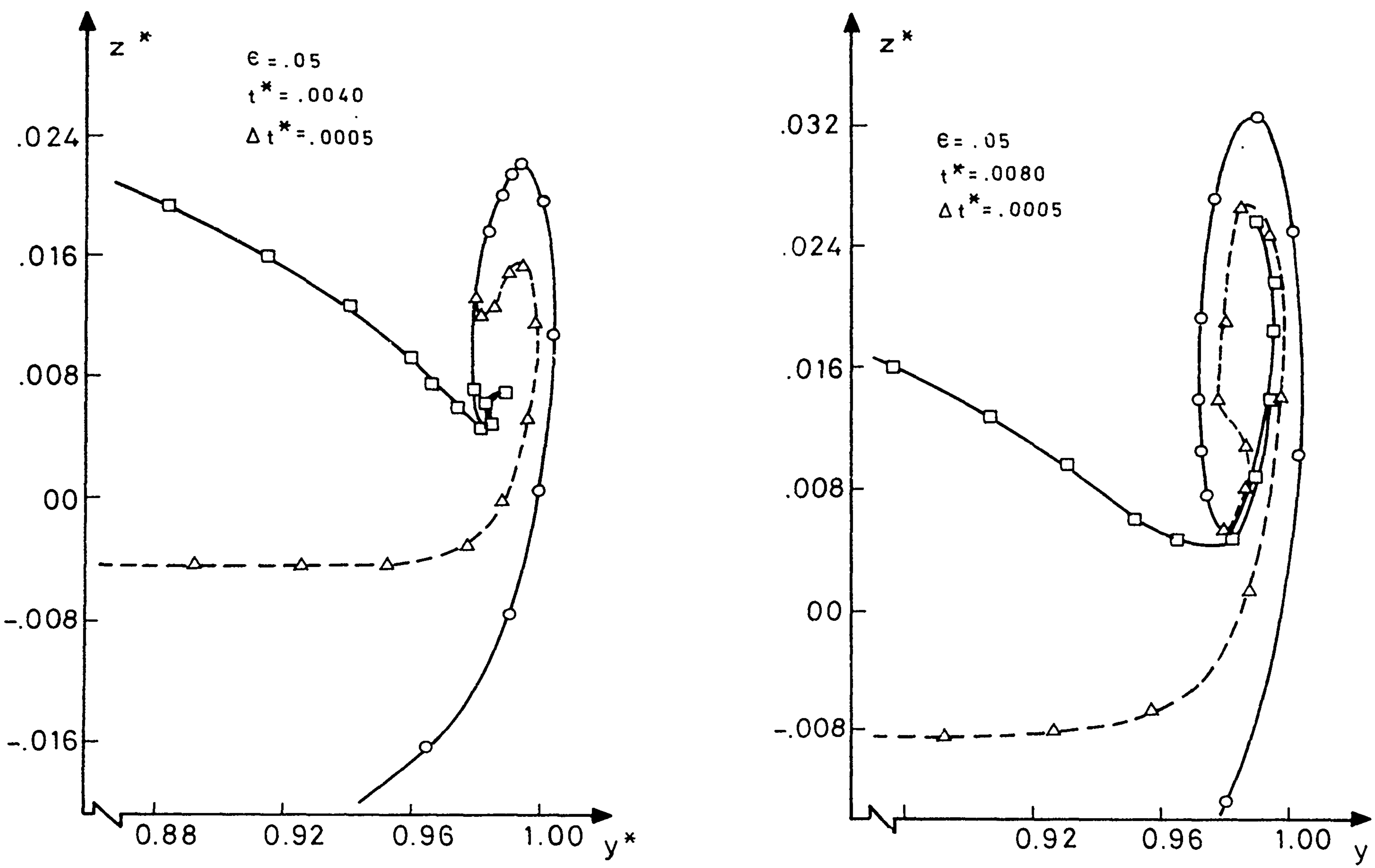
z*
ϵ = .05
t* = .0040
Δt* = .0005
.024
.016
.008
00
-.008
-.016
0.88
0.92
0.96
1.00
y*
z*
ϵ = .05
t* = .0080
Δt* = .0005
.032
.024
.016
.008
00
-.008
0.92
0.96
1.00
y*

FIG. 5

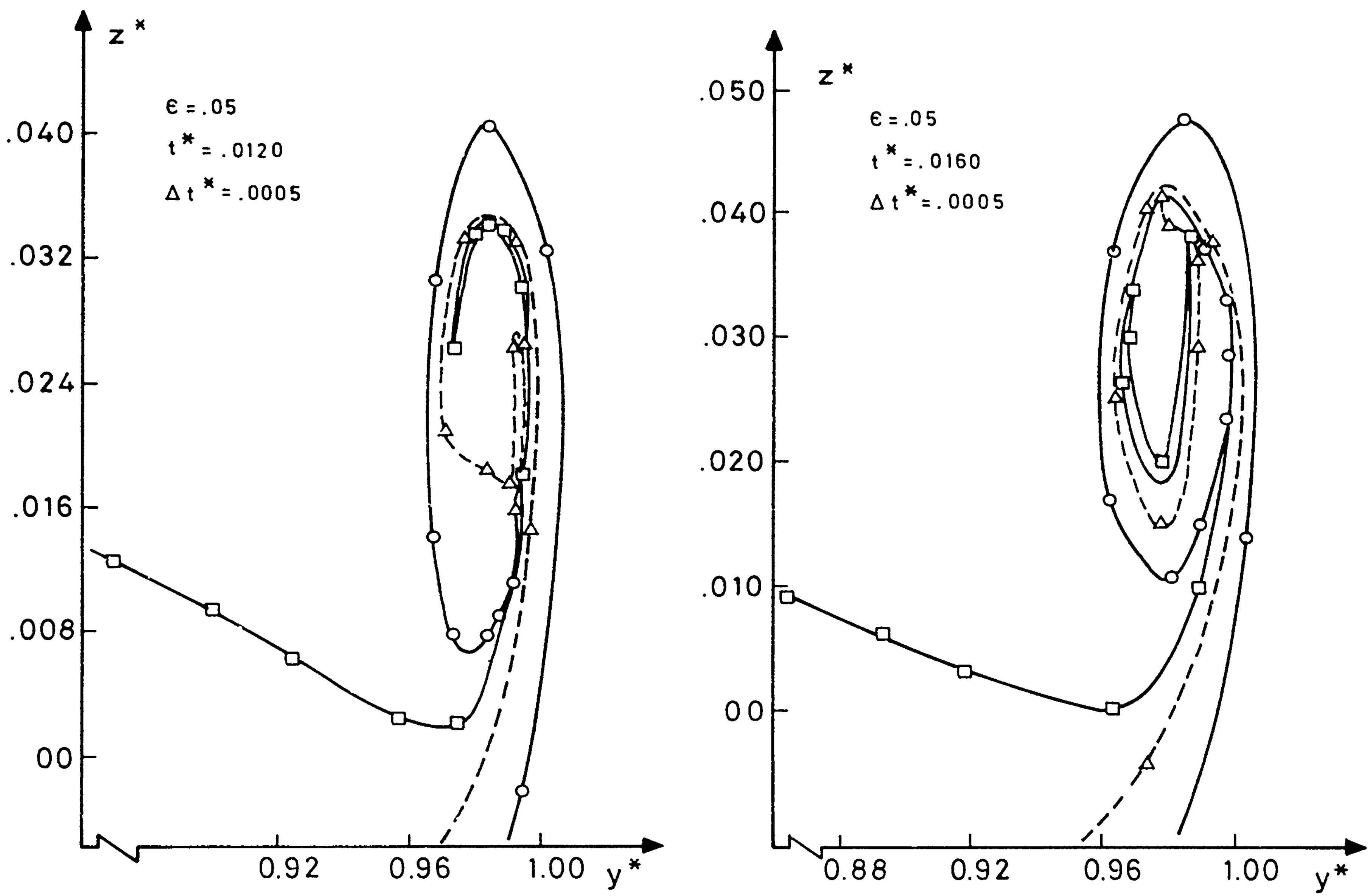

z*
ϵ = .05
t* = .0120
Δt* = .0005
.040
.032
.024
.016
.008
00
0.92
0.96
1.00
y*
z*
ϵ = .05
t* = .0160
Δt* = .0005
.050
.040
.030
.020
.010
00
0.88
0.92
0.96
1.00
y*

FIG. 5 CONT.

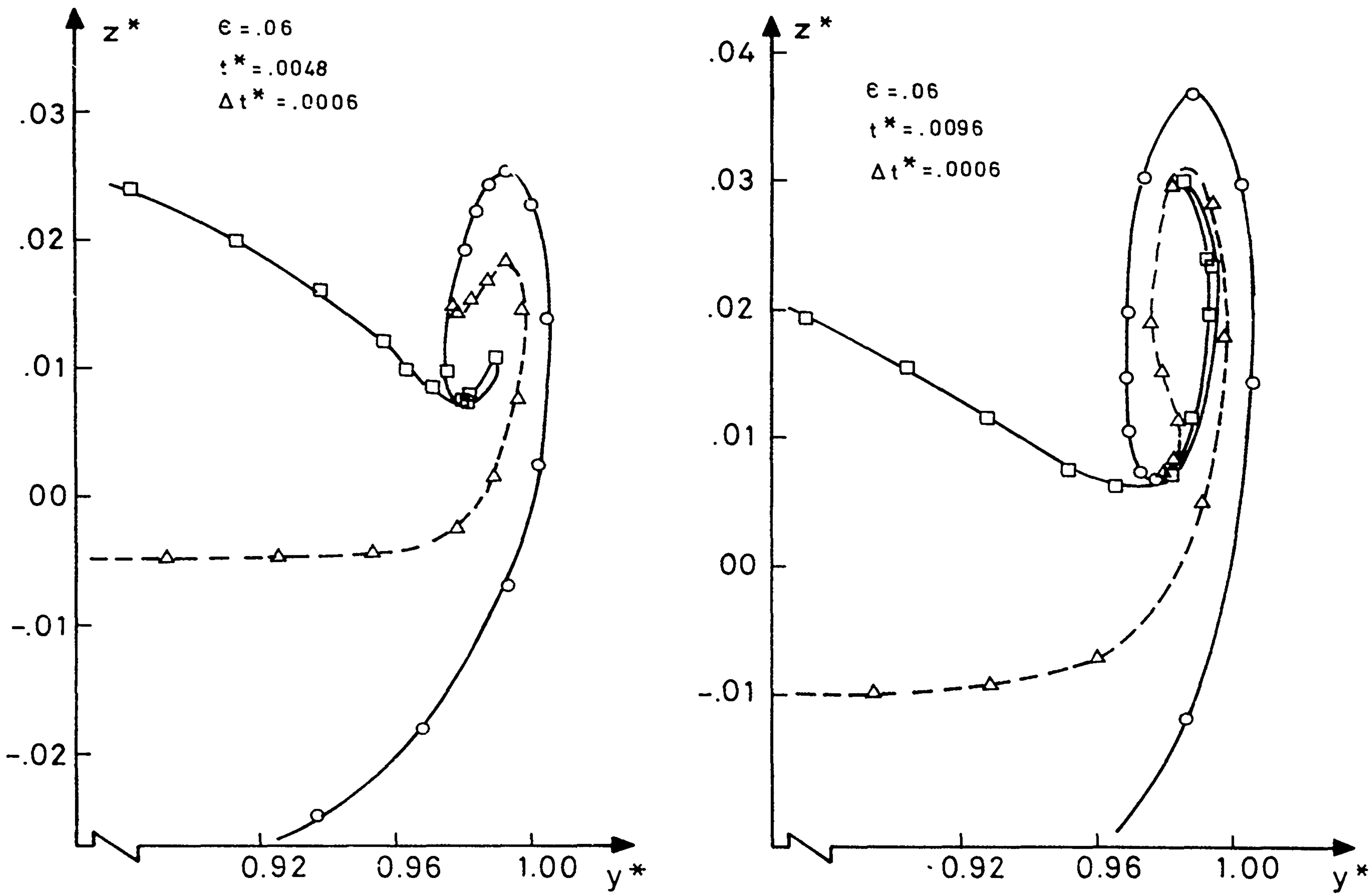

z*
ε = .06
t* = .0048
Δt* = .0006
.03
.02
.01
00
-.01
-.02
0.92
0.96
1.00
y*
z*
.04
ε = .06
t* = .0096
Δt* = .0006
.03
.02
.01
00
-.01
0.92
0.96
1.00
y*

FIG. 6

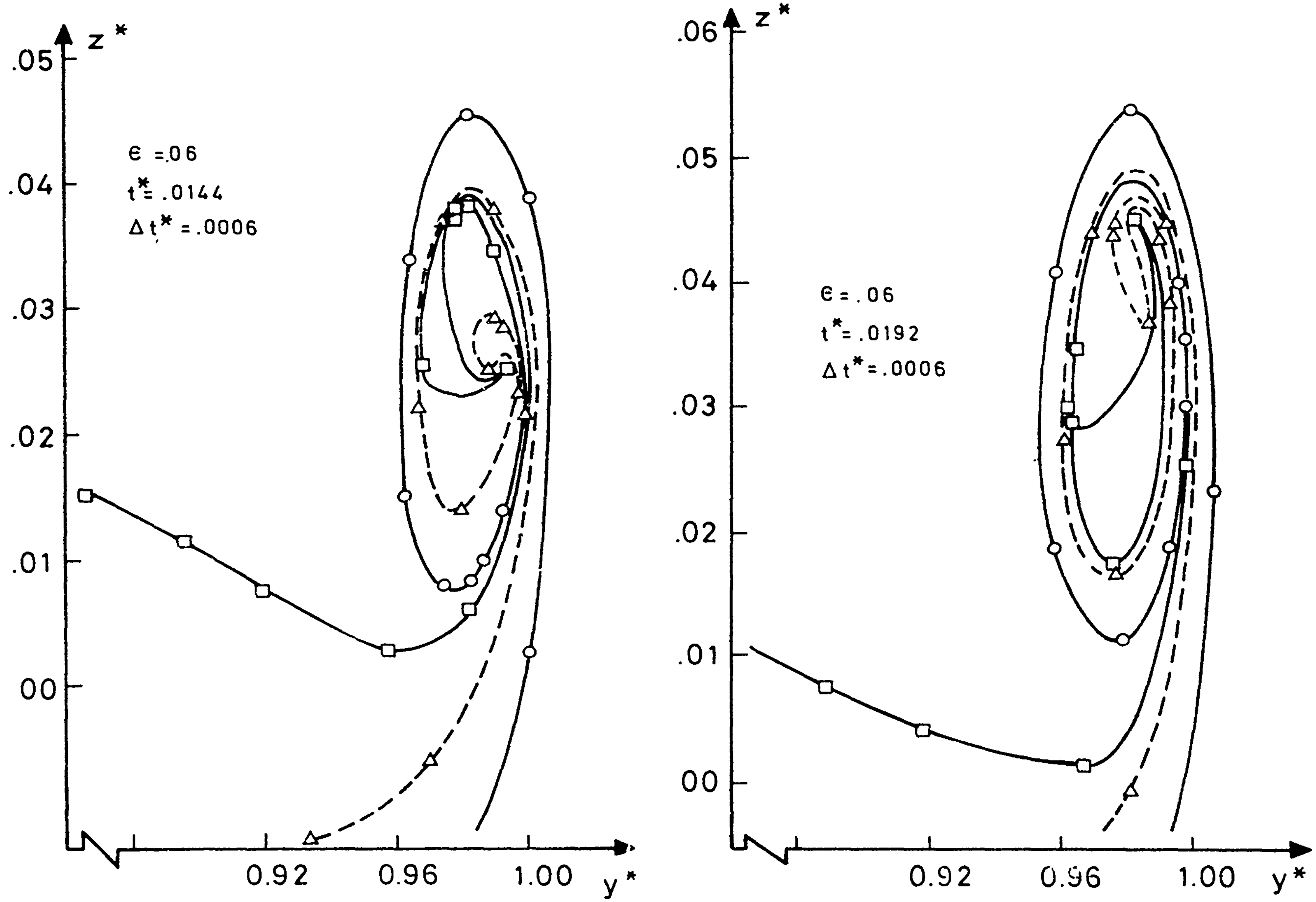

ϵ =.06
t^*= .0144
Δt^* = .0006
z^*
y^*
.05
.04
.03
.02
.01
00
0.92
0.96
1.00
ϵ = .06
t^*= .0192
Δt^* = .0006
.06

FIG. 6 CONT.

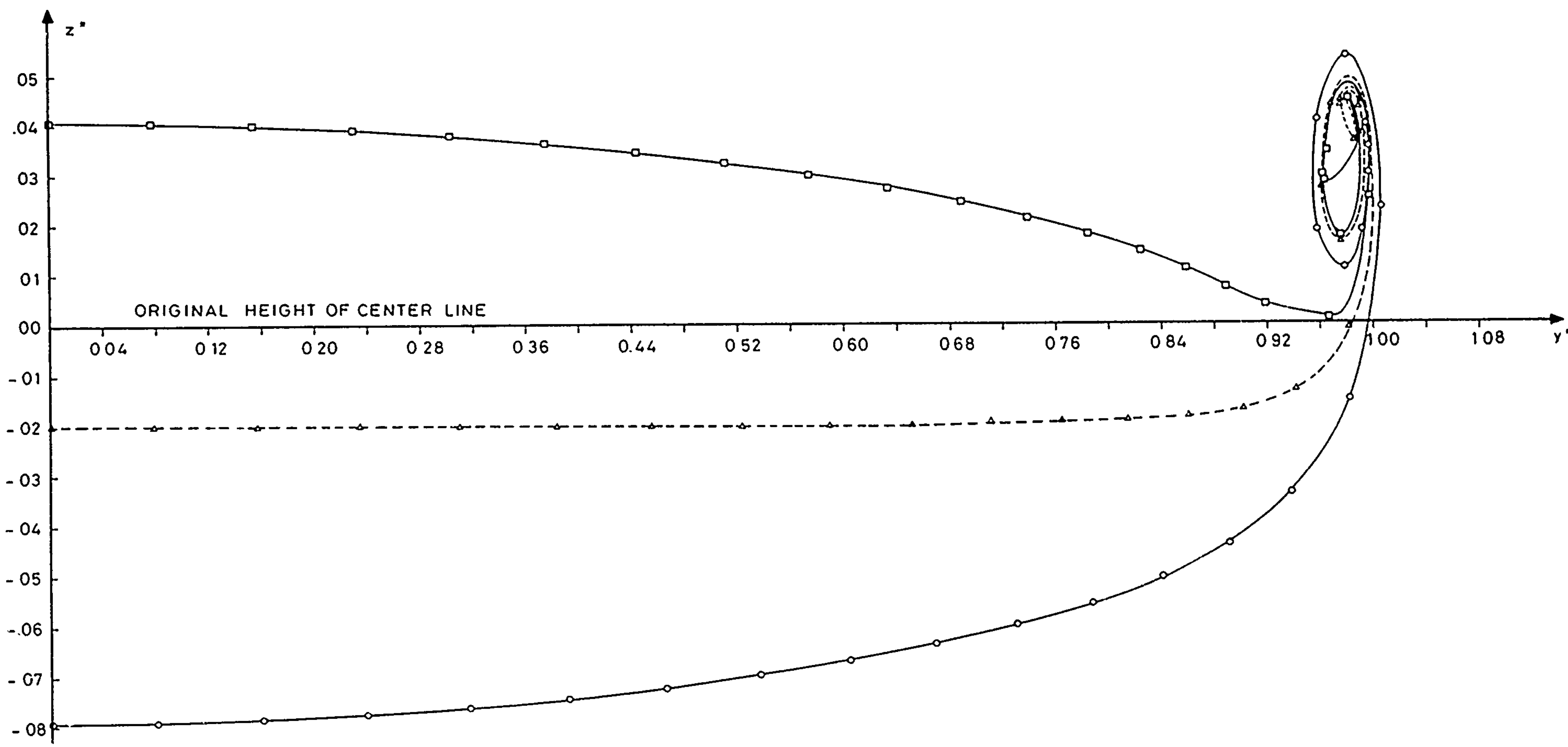

$\epsilon = 06 \qquad t^{*} = 0192 \qquad \Delta t^{*} = 0006$

FIG 7 - EXAMPLE OF A COMPLETE HALF WAKE

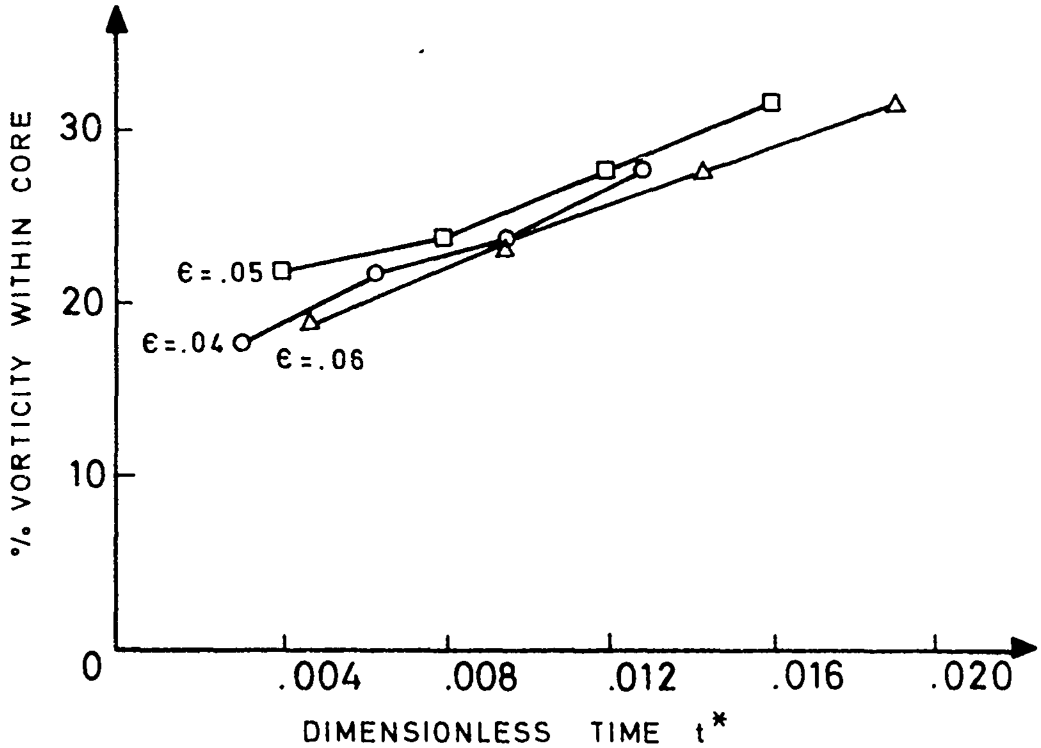

% VORTICITY WITHIN CORE
30
20
10
0
ϵ = .05
ϵ =.04
ϵ = .06
.004
.008
.012
.016
.020
DIMENSIONLESS TIME t*

FIG. 8

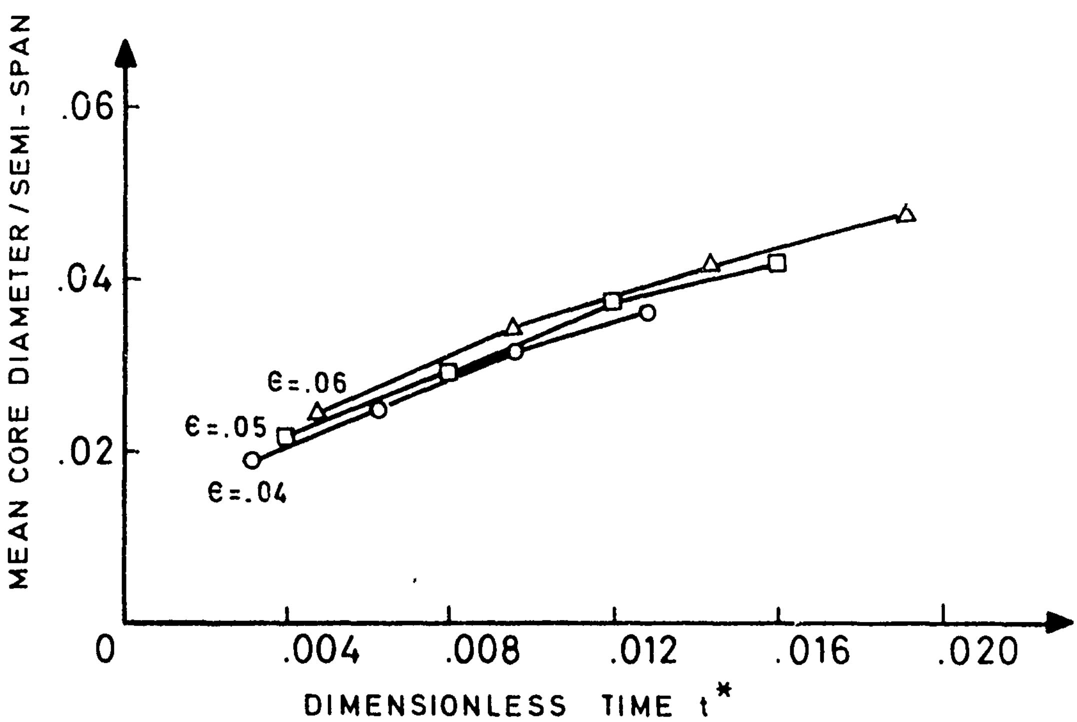

MEAN CORE DIAMETER / SEMI - SPAN
.06
.04
.02
0
ϵ =.06
ϵ =.05
ϵ =.04
.004
.008
.012
.016
.020
DIMENSIONLESS TIME t*

FIG. 9

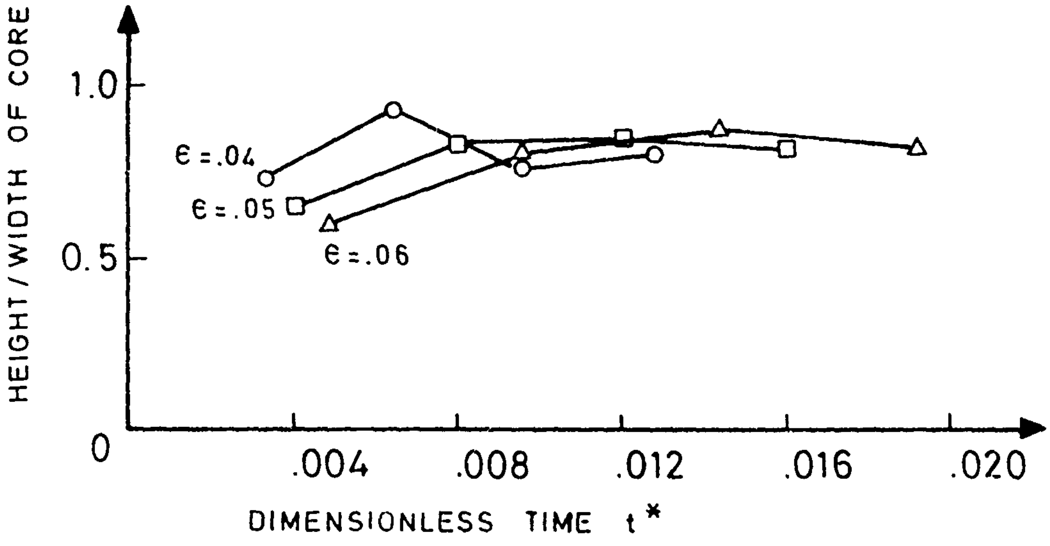
HEIGHT / WIDTH OF CORE
1.0
0.5
0
ε = .04
ε = .05
ε = .06
.004
.008
.012
.016
.020
DIMENSIONLESS TIME t*

FIG.10

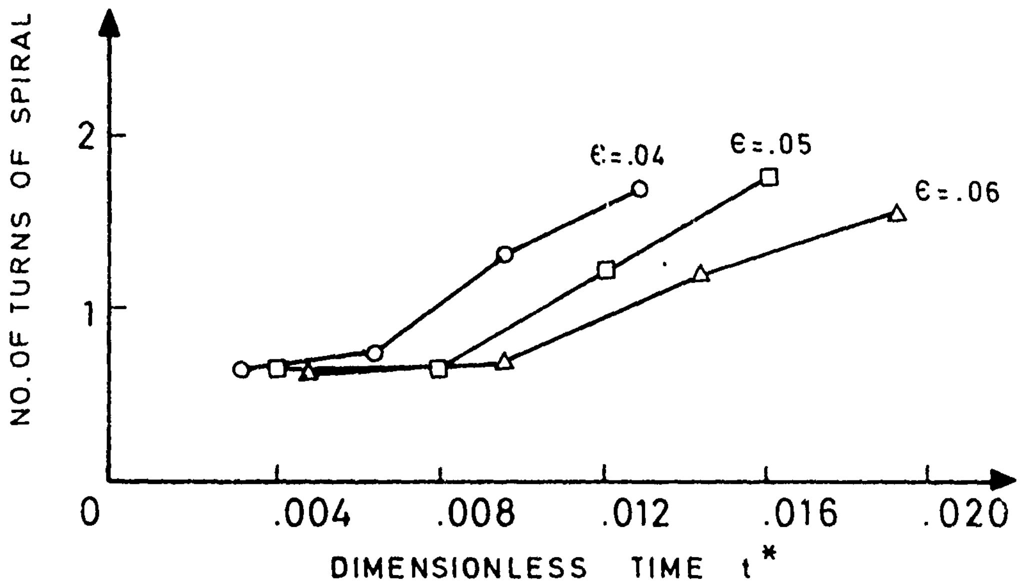
NO. OF TURNS OF SPIRAL
2
1
0
ε = .04
ε = .05
ε = .06
.004
.008
.012
.016
.020
DIMENSIONLESS TIME t*

FIG. 11

UNCLASSIFIED

SECURITY CLASSIFICATION OF THIS PAGE (When Data Entered)

REPORT DOCUMENTATION PAGE		READ INSTRUCTIONS BEFORE COMPLETING FORM
1. REPORT NUMBER 18 19 AFOSR - TR - 76 - 0382	2. GOVT ACCESSION NO.	3. RECIPIENT'S CATALOG NUMBER 9
4. TITLE (and Subtitle) 6 THE INITIAL ROLL-UP OF A THICK, TWO-DIMENSIONAL WAKE BEHIND A WING OF FINITE SPAN,		5. TYPE OF REPORT & PERIOD COVERED INTERIM rept.,
		6. PERFORMING ORG. REPORT NUMBER Report No 7
7. AUTHOR(s) 10 H. PORTNOY		8. CONTRACT OR GRANT NUMBER(s) 15 AF-AFOSR-2145-71
9. PERFORMING ORGANIZATION NAME AND ADDRESS TECHNION - ISRAEL INSTITUTE OF TECHNOLOGY DEPARTMENT OF AERONAUTICAL ENGINEERING HAIFA, ISRAEL		10. PROGRAM ELEMENT, PROJECT, TASK AREA & WORK UNIT NUMBERS 681307 16 AF-9781-01 17 978101 61102F
11. CONTROLLING OFFICE NAME AND ADDRESS AIR FORCE OFFICE OF SCIENTIFIC RESEARCH/NA BUILDING 410 BOLLING AIR FORCE BASE, D C 20332		12. REPORT DATE 11 Nov 75
		13. NUMBER OF PAGES 35 12 38p.
14. MONITORING AGENCY NAME & ADDRESS (if different from Controlling Office) 14 TAE-262, Scientific-7		15. SECURITY CLASS. (of this report) UNCLASSIFIED
		15a. DECLASSIFICATION/DOWNGRADING SCHEDULE

16. DISTRIBUTION STATEMENT (of this Report)

Approved for public release; distribution unlimited.

17. DISTRIBUTION STATEMENT (of the abstract entered in Block 20, if different from Report)

18. SUPPLEMENTARY NOTES

19. KEY WORDS (Continue on reverse side if necessary and identify by block number)

WING WAKES
ROLLING-UP
VORTICITY DISTRIBUTIONS
INDUCED VELOCITY
NUMERICAL TECHNIQUE

20. ABSTRACT (Continue on reverse side if necessary and identify by block number)

Previous investigations of wing-wake roll-up have assumed the wake to be a vortex sheet of zero thickness. This immediately leads to the conclusion that, as soon as the process starts, a spiral of near axisymmetric form, with an infinite number of turns, forms at the edges, as predicted by the work of Kaden, which must apply to the early stages of roll-up for any sheet of zero thickness. In addition, most investigators, starting with Westwater, have replaced the continuous vortex sheet by discrete vortex lines. In this report, the aforementioned unrealistic features are removed by assuming that the wake

DD FORM 1 JAN 73 1473 EDITION OF 1 NOV 65 IS OBSOLETE

UNCLASSIFIED 343 875

SECURITY CLASSIFICATION OF THIS PAGE (When Data Entered) cross-section has a finite thickness and some plausible shape. A two-dimensional method, analogous to that of Westwater, is developed, assuming that the wake cross-section contains vorticity in an otherwise irrotational field. The wake is divided into triangular elements and the vorticity in these is determined by assuming a linear transverse velocity profile in the wake and that the initial, unrolled wake moves downwards as determined by the wing spanwise loading through ordinary wing-wake theory. Euler time-step integration is then used to calculate the wake development under its own induced velocity field, ignoring viscous dissipation. Three examples of the initial stages of roll-up, for elliptic wakes of thickness ratios .04 .05 and .06 are calculated. A finite spiral structure is observed to develop and, within the range covered, the thickness only seems to affect the number of turns in the spiral, other parameters seeming to be almost unaffected. Plans for continuation of the work are discussed.